

## Effects of straight groin parameters on amount of accretion

Ismail Hakkı Özölçer<sup>1\*</sup> & Murat İhsan Kömürçü<sup>2</sup>

<sup>1</sup>Zonguldak Karaelmas University, Civil Engineering Dept., 67100 Zonguldak, Turkey

<sup>2</sup>Karadeniz Technical University, Civil Engineering Dept., 61080 Trabzon, Turkey

\*[E-mail:ozolcer@hotmail.com]

Received 17 April 2006; revised 14 May 2006

Various types of structures are used in shore protection and littoral sediment trapping. Groins are one of these structures. The main hydraulic function of the groin is to control the long shore current and littoral sediment transport. In this paper, the effects of various groin parameters (length and spacing) and wave parameters (wave height, wave period and wave angle) on the accretion of the area protected by straight groin were studied in a physical model. The model studies were performed using regular waves in a basin. A numerical model which depends primarily on a CERC model is employed to examine the effects of some of the above parameters. Good agreement was found in the results of physical and numerical models. The results of a numerical model are compared with field data that were obtained by deep sounding measurements at Çarşıbaşı coasts, Trabzon Province, Turkey. The important outcome from this study may be employed in designing of straight groins.

**[Key words:** Straight groins, shore protection, sediment transport, accretion parameter, numerical model, field data]

### 1. Introduction

A groin is a shore protection structure designed to trap littoral drift and, to some extent, the cross-shore sediment for creating a protective beach, retarding erosion of an existing beach, or preventing long shore drift from reaching some down drift point, such as a harbor or inlet. Groins are narrow structures with variable lengths and heights and are usually constructed in perpendicular to shoreline. Groins can be constructed as a single structure or in series (groin field).

Several investigations have been conducted in the past to study the effects of groin parameters on shoreline change<sup>1-8</sup>. Some of the most important studies are summarized as follows:

Price & Tomlinson<sup>1</sup> conducted a study on the effects of groins on stable beaches and studied the coastal changes for various groin parameters, using a three-dimensional physical model. Barcelo<sup>2</sup> studied an experimental investigation of the hydraulic behavior of groin systems and researched the problems of sediment trapping and erosion for various groin spacing. Hanson & Kraus<sup>3</sup> experimentally investigated the effects of a series of three groins on

shore evolution and proposed a numerical model (GENESIS) and concluded that this model was in agreement with the results of the physical model. Kraus *et al.*<sup>4</sup> carried out physical model studies on groin parameters and proposed that groin length may be equal to groin opening. Badici *et al.*<sup>5</sup> investigated the effects of groins on shore, using a three-dimensional physical model. Güngördü & Otay<sup>6</sup> proposed a numerical model to calculate the shoreline changes in the vicinity of a groin employing only long shore sediment transport and compared their model with field data. Leont'yev<sup>7</sup> suggested a numerical model to simulate the short-term temporal changes in shoreline position due to a structure interrupting the long shore sediment transport. Özölçer *et al.*<sup>8</sup> studied the effects of T-shaped groin parameters on the accretion in a physical model in three-dimensional wave basin using regular waves. They also carried out a numerical model about shoreline changes. The results of a numerical model are compared with field data.

In the present study, the effects of various groin parameters on the accretion of the area protected by straight groins are studied both by physical and numerical models. The results of a numerical model are compared with field data that were obtained by deep sounding measurements at Çarşıbaşı Coasts,

\*Corresponding author  
Fax: +90-372-2574023  
Tel.: +90-372-2574010

Trabzon Province, Turkey. The dominant wave direction of the location varies from NW to N, causing net littoral transport from west to east<sup>9</sup>. The developed numerical model computes the evolution of bed contours depending on both long shore and cross-shore sediment transport rates.

**2. Materials and Methods**

**2.1. Experimental studies**

**2.1.1. Model basin**

Physical model studies were performed at the Karadeniz Technical University, using a wave basin with 30×12×1.5 m. An undistorted model scale of 1/75 was selected by taking into account the dimensions of the basin and an average groin. The slope of the model bed was 1/25 and the bed<sup>10</sup> material was fine sand ( $d_{50}=0.16$  mm). Determination of material properties in the proposed model was considered as a significant problem. There has been a certain method to choose model scaling of bed material although several investigations have been carried out recently. On the contrary to that material with different densities are proposed in experimental and theoretical works. Thus, it is not possible to determine which material, in nature, would correspond to the fine sand used. However in the laboratory, the bed material was easily transported by waves, and it was assumed that its qualitative movement was representative of the prototype.

The model basin (Fig. 1) has a wave-generator system, a speed control system, and a wave-height measurement system for the generation and measurement of waves. Monochromatic wave height and wave period were controlled by a screwed handle and by a speed control. An electronic wave gauge was used to measure the wave heights in and wave period was measured using a chronometer. The bed material (sand) was spread over the basin bed. The waves having an angle  $\alpha$  to the shoreline cause littoral sediment transport. To represent these waves, taking into consideration the restrictions imposed by the basin dimensions, a maximum wave angle about  $\alpha_0=30^\circ$  was chosen for the deep-water waves. The groins were constructed of stone blocks and separated by iron sheets. The sheet irons were sunk into the bed in order to make groins impermeable to both the waves and sediment.

The model zone was divided by 25×25 cm grids. Within each grid, elevations of the sandy surface in the basin, before and after an experiment ( $h_1$  and  $h_2$ , respectively), were measured using a ruler and the

accumulation height was determined by  $\Delta h=h_2-h_1$ . Preliminary experiments showed that a testing period of  $t=240$  min (35 hr in prototype) was sufficient; at the end of this period, the shoreline reached an equilibrium.

**2.1.2. Tested parameters**

The tested groin parameters were the groin length ( $L_x$ ) and spacing between successive groins ( $L_G$ ) (Fig. 2). All of the tested groin and wave parameters are given in Table 1. The significant wave parameters were obtained from the Eastern Black Sea wave climate<sup>8,10</sup>.

**2.1.3. Analysis of experimental results**

Experimental data were analyzed using two groin parameters, groin length ( $L_x$ ) and spacing between successive groins ( $L_G$ ), which were identified from previous study<sup>8,10</sup>. A dimensionless accretion

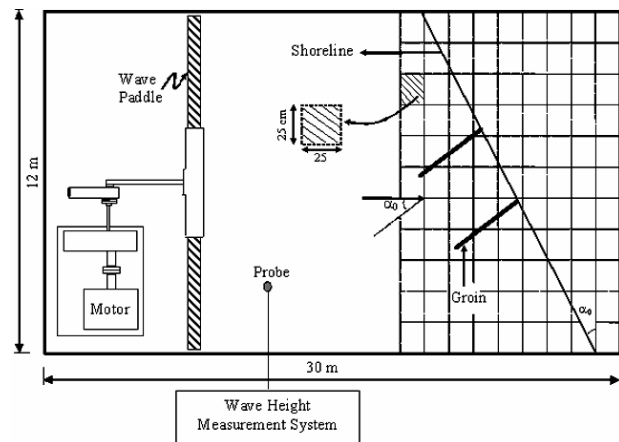


Fig. 1—Experimental set-up and measurement system in a wave basin

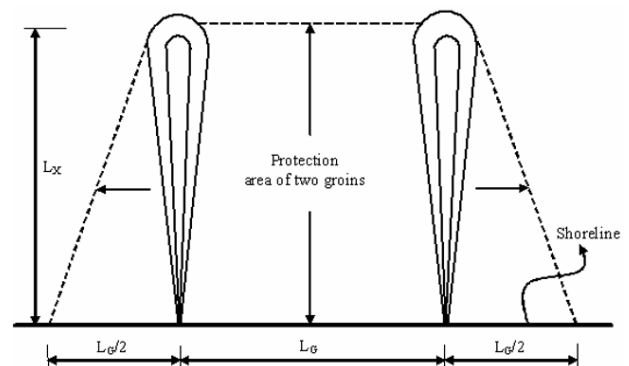


Fig. 2—Tested groin parameters and groins protection area

parameter is defined as follows (Fig. 3):

$$R = \frac{D \times A_s}{A_G \times h_m} = \frac{D \times A_s}{n \times A_s \times h_m} = \frac{D}{n \times h_m} \quad \dots (1)$$

where, D is the total accretion height within the groin area; A<sub>s</sub> is the area of a grid in the measuring grid system (625 cm<sup>2</sup>); A<sub>G</sub> is the total area protected by groins, h<sub>m</sub> is the depth of head of the groin and n is total measuring point. The total area protected by

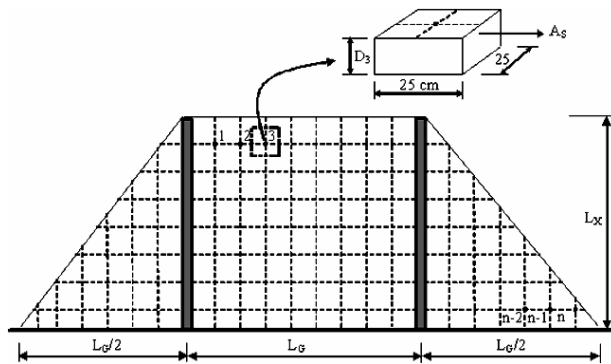


Fig. 3—Defining of groin measurement area

groin is calculated several geometrical dimensions of the groin,

$$A_G = \frac{\left[ L_G + L_G + \frac{L_G}{2} + \frac{L_G}{2} \right] \times L_X}{2} \quad \dots (2)$$

$$= \frac{(3 \times L_G) \times L_X}{2} = \frac{3}{2} \times L_G \times L_X$$

All of the R values obtaining from tests are given in Table 1.

2.2. Numerical model studies

2.2.1. General

In addition to the physical model studies, numerical model studies were also performed and their results compared with each other.

There are a number of numerical models on shoreline changes, which have been cited in the literature. Among them, one-line model, which considers only the shoreline change, and n-line model that takes into account the changes of bed contours are the most well known models. Since both cross-shore and long-shore sediment transport are dominant

Table 1—Tested parameters and R values

Test No	m	α (°)	T (sec.)	H (cm)	h <sub>m</sub> (cm)	H/L	L <sub>X</sub> (cm)	L <sub>G</sub> (cm)	R
1	1/25	30	0.866	3.33	4.00	0.028	100.00	100.00	0.1073
2	1/25	30	0.866	3.33	4.00	0.028	100.00	130.00	0.1323
3	1/25	30	0.866	3.33	4.00	0.028	100.00	170.00	0.1258
4	1/25	30	0.866	3.33	4.00	0.028	100.00	200.00	0.1328
5	1/25	30	0.866	3.33	4.00	0.028	100.00	230.00	0.1125
6	1/25	30	0.866	3.33	4.00	0.028	100.00	260.00	0.0638
7	1/25	15	0.866	3.33	4.00	0.028	100.00	100.00	0.1450
8	1/25	15	0.866	3.33	4.00	0.028	100.00	130.00	0.1120
9	1/25	15	0.866	3.33	4.00	0.028	100.00	170.00	0.1200
10	1/25	15	0.866	3.33	4.00	0.028	100.00	200.00	0.0828
11	1/25	15	0.866	3.33	4.00	0.028	100.00	230.00	0.0278
12	1/25	15	0.866	5.33	4.00	0.045	100.00	130.00	0.0300
13	1/25	15	0.866	5.33	4.00	0.045	100.00	170.00	0.0450
14	1/25	15	0.866	5.33	4.00	0.045	100.00	200.00	0.0365
15	1/25	15	0.866	5.33	4.00	0.045	100.00	230.00	0.0370
16	1/25	15	0.692	3.33	4.00	0.045	100.00	130.00	0.0080
17	1/25	15	0.692	3.33	4.00	0.045	100.00	170.00	-0.0035
18	1/25	15	0.692	3.33	4.00	0.045	100.00	200.00	-0.0098
19	1/25	15	0.692	3.33	4.00	0.045	100.00	260.00	-0.0303
20	1/25	15	0.866	3.33	5.33	0.028	133.33	133.33	0.06470
21	1/25	15	0.866	3.33	5.33	0.028	133.33	173.33	0.04290
22	1/25	15	0.866	3.33	5.33	0.028	133.33	226.67	0.04140
23	1/25	15	0.866	3.33	5.33	0.028	133.33	266.67	0.03190
24	1/25	15	0.866	3.33	5.33	0.028	133.33	346.67	0.00994

m (bed slope), α (deep sea wave angle), T (wave period), H (deep sea wave height)

on a coast with straight groins, a three-dimensional numerical model should be employed to compute the changes to contour<sup>11-13</sup>. In this study, a numerical model considering each point of bed topography was developed.

In Fig. 4, x-axis is shoreline, y-axis is perpendicular to shore and z-axis is the water depth.

$$\Delta V = \Delta X \cdot \Delta Y \cdot \Delta Z \quad \dots (3)$$

$$\Delta V = \Delta Q \cdot \Delta t \quad \dots (4)$$

$$\Delta Z = \frac{\Delta V}{\Delta X \cdot \Delta Y} = \frac{\Delta Q \cdot \Delta t}{\Delta X \cdot \Delta Y} \quad \dots (5)$$

where, V is volume of unit component; X, Y and Z are dimensions, Q is sediment discharge and t is time. If Eq. 5 is written for each i grid, it can be arranged as follow:

$$\Delta Z_i = \frac{\Delta Q_i \cdot \Delta t}{\Delta X_i \cdot \Delta Y_i} \quad \dots (6)$$

For the small i intervals,  $\Delta x \rightarrow \partial x$ ,  $\Delta y \rightarrow \partial y$  and  $\Delta t \rightarrow \partial t$ ,

$$\frac{\partial z}{\partial t} = \frac{\partial q_y}{\partial x} + \frac{\partial q_x}{\partial y} \quad \dots (7)$$

Equation 7 is the main equation in variation of bed topography and is called continuity equation<sup>13</sup>. Where t is time;  $q_x$  and  $q_y$  are x (longshore) and y (cross-shore) components of sediment transport discharge, and x, y and z are Cartesian coordinates. Finite difference method is used to solve the continuity equation in this study.

A number of studies were performed on the point where the transport discharge is maximum,  $q_x/q_{max}=1.0$ . In Watanabe's equation<sup>14</sup>  $0.53 < x/x_b < 0.85$ , with an average value of  $x/x_b=0.7$ , where x and  $x_b$  are distances of the points of interest and breaking from shoreline, respectively. CERC equation<sup>15,16</sup> proposed that maximum transport would be at  $x/x_b=0.7$ .

Taking into consideration the above proposals, three kinds of models were employed in this study;  $x/x_b=0$ ,  $x/x_b=0.5$  and  $x/x_b=0.7$ . The resulting equations for the sediment transport at these three locations are given<sup>8</sup> as follows:

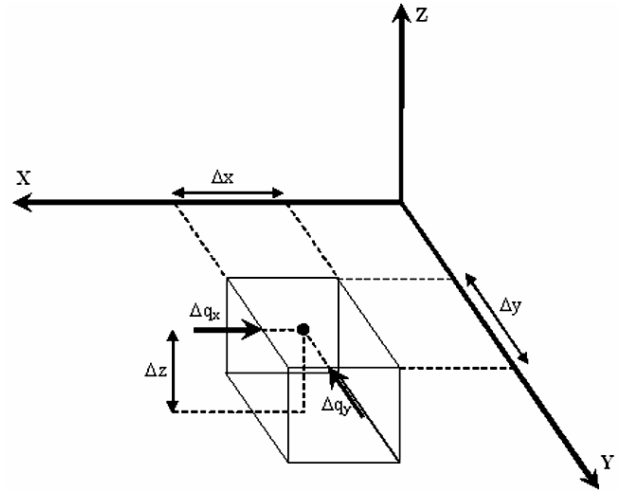


Fig. 4—Depiction of the numerical model

$$\text{For } x/x_b=0 \Rightarrow q(x/x_b) = [1.25 - 0.7875 \cdot (x/x_b)^{2/3}] \cdot Q_x \quad \dots (8)$$

$$\text{For } x/x_b=0.5 \Rightarrow q(x/x_b) = Q_x \cdot 11.35 \cdot (x/x_b + 0.5)^{4.9} \cdot e^{-5 \cdot x/x_b} \quad \dots (9)$$

$$\text{For } x/x_b=0.7 \Rightarrow q(x/x_b) = Q_x \cdot 0.98 \cdot (x/x_b + 0.825)^{7.1} \cdot e^{-4.7 \cdot x/x_b} \quad \dots (10)$$

In these equations  $Q_x$  is longshore sediment transport discharge and will be explained in the following section.

2.2.2. Sediment transport rate

There are numerous formulae to predict both cross-shore and long shore sediment transport rate. By analyzing these formulae, the following two equations used in this study were employed:

For cross-shore transport rate the formula is given by Watanabe<sup>14</sup>;

$$Q_y = 7 \cdot w_o \cdot d \cdot (\psi_m - \psi_c) \cdot \psi^{0.5} \quad \dots (11)$$

$$\psi_m = \frac{\tau_b}{\rho s g d}, \quad \Psi = \frac{(d\sigma)^2}{s g d}, \quad \sigma = \frac{2\pi}{T}$$

where T is wave period,  $\tau_b$  is bed shear stress, s is weight of sediment in water, d is diameter of sediment,  $\rho$  is density of water;  $\psi_c$  is critic shields parameter,  $w_o$  is settling velocity of the sediment particle and g is acceleration due to gravity.

For long shore transport rate formulae are as follows<sup>15,17</sup>:

$$Q_x = (H^2 C_g)_b \left[ a_1 \sin(2\alpha_b) - a_2 \cos(\alpha_b) \frac{\partial H}{\partial x} \right] \dots (12)$$

$$C_g = \left( \frac{g H_b}{\phi} \right)^{0.5}$$

$$a_1 = \frac{K_1}{[16(\gamma_s/\gamma - 1)(1 - p)1.416^{2.5}]}$$

$$a_2 = \frac{K_2}{[8(\gamma_s/\gamma - 1)(1 - p)1.416^{3.5} \tan \beta]}$$

where  $\alpha$  is wave angle,  $\phi$  is the breaking index ( $H_b/h_b$ ),  $\gamma$  and  $\gamma_s$  are specific gravity of water and sediment particles respectively,  $p$  is porosity of sediment particles,  $\tan \beta$  is bed slope,  $K_1$  and  $K_2$  are empirical coefficients ( $0.58 \leq K_1 \leq 0.77$ ,  $0.5K_1 \leq K_2 \leq K_1$ ) and subscript  $b$  denotes wave breaking point.

Kamphuis<sup>18</sup> proposed a different formula:

$$Q_x = 0.00203 H_b^2 T^{1.5} m^{0.75} d_{50}^{-0.25} [\sin(2\alpha_b)]^{0.6} \dots (13)$$

**2.2.3. Execution of the numerical model**

By using Eqs. 7-13, a numerical scheme was developed to compute the bed changes. The studied area was divided into 12.5×12.5 cm grids. Positive directions of  $Q_x$  (long shore) and  $Q_y$  (cross-shore) values are given in Fig. 5. Wave breaking height in the model was computed by<sup>15</sup>:

$$K = b - a \frac{H_b}{gT^2} \dots (14)$$

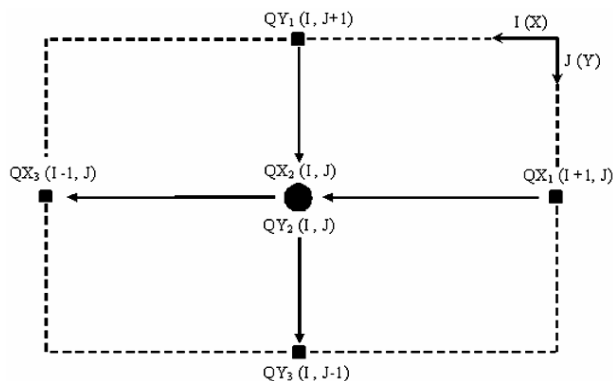


Fig. 5—Positive directions of sediment transport in the numerical model

$$H_b = K h_b, a = 43.75(1 - e^{-19m}), b = \frac{1.56}{(1 + e^{-19.5m})}$$

where,  $m$  is the bed slope ( $\tan \beta$ ). Shoaling ( $K_s$ ) and refraction ( $K_r$ ) coefficients were calculated by assuming bed contours parallel to the shore. In calculating diffraction coefficient ( $K_D$ ) at the gap of two straight groins,  $K_D$  values of each groin were multiplied<sup>8,10</sup>. Numerical model results are given in Table 2.

**2.3. Field study**

The field study was carried out at a location at Çarşıbaşı (a town 50 km west of Trabzon Province) Coast in which there was a straight groin<sup>19</sup>. There was a single straight groin with 100 m length. At the beginning of the measurements, the bed contours were roughly straight and parallel to the shoreline; the depth at the outer part of the head was 2 m, which means that the average bed slope was 1/30. The bed contours were measured four times in a year. The shorelines, obtained from field study and numerical model, are given in Fig. 6.

**3. Results**

**3.1. Evaluation of physical model results**

In this section, the effects of various groin ( $L_G$  and  $L_X$ ) and wave parameters ( $H_0$ ,  $T$ , and  $\alpha_0$ ) on the dimensionless accretion parameter ( $R$ ) are discussed.

**3.1.1. Effect of groin length ( $L_X$ )**

In order to study the effect of groin length on the accretion parameter; totally 10 experiments were performed. In these experiments;  $H$  and  $T$ , were kept constant as 3.33 cm and 0.866 sec. respectively. Then two  $L_X$  values (100 and 133.3) were chosen and ten

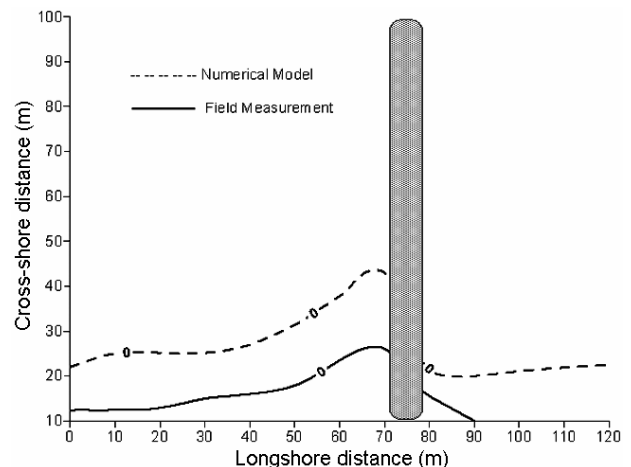


Fig. 6—The shoreline change (12 months later from construction)

Table 2—Numerical model results

Test No	H (cm)	T (sec.)	$\alpha$ (°)	$\frac{H}{L}$	$L_x$ (cm)	$\frac{L_G}{L_x}$	Cerc			Kamphuis
							$\frac{X}{X_b}=0$	$\frac{X}{X_b}=0.5$	$\frac{X}{X_b}=0.7$	$\frac{X}{X_b}=0$
1	3.33	0.866	30	0.028	100	1.0	0.136	0.092	0.066	0.120
2	3.33	0.866	30	0.028	100	1.3	0.184	0.092	0.061	0.188
3	3.33	0.866	30	0.028	100	1.7	0.129	0.054	0.032	0.136
4	3.33	0.866	30	0.028	100	2.0	0.134	0.055	0.031	0.160
5	3.33	0.866	30	0.028	100	2.3	0.12	0.049	0.025	0.154
6	3.33	0.866	30	0.028	100	2.6	0.105	0.042	0.024	0.140
7	3.33	0.866	15	0.028	100	1.0	0.121			
8	3.33	0.866	15	0.028	100	1.3	0.115			
9	3.33	0.866	15	0.028	100	1.7	0.074			
10	3.33	0.866	15	0.028	100	2.0	0.069			
11	3.33	0.866	15	0.028	100	2.3	0.061			
-	3.33	0.866	15	0.028	100	2.6	0.054			
-	3.33	0.866	15	0.028	100	1.0	0.129			
12	5.33	0.866	15	0.045	100	1.3	0.177			
13	5.33	0.866	15	0.045	100	1.7	0.120			
14	5.33	0.866	15	0.045	100	2.0	0.154			
15	5.33	0.866	15	0.045	100	2.3	0.158			
-	5.33	0.866	15	0.045	100	2.6	0.134			
-	5.33	0.866	15	0.045	100	1.0	0.110			
16	3.33	0.692	15	0.045	100	1.3	0.103			
17	3.33	0.692	15	0.045	100	1.7	0.066			
18	3.33	0.692	15	0.045	100	2.0	0.060			
-	3.33	0.692	15	0.045	100	2.3	0.054			
19	3.33	0.692	15	0.045	100	2.6	0.047			
-	3.33	0.866	30	0.028	67	1.0	0.136			
-	3.33	0.866	30	0.028	67	1.3	0.129			
-	3.33	0.866	30	0.028	67	1.7	0.083			
-	3.33	0.866	30	0.028	67	2.0	0.077			
-	3.33	0.866	30	0.028	67	2.3	0.068			
-	3.33	0.866	30	0.028	67	2.6	0.061			
-	3.33	0.866	15	0.028	120	1.0	0.111			
-	3.33	0.866	15	0.028	120	1.3	0.106			
-	3.33	0.866	15	0.028	120	1.7	0.068			
-	3.33	0.866	15	0.028	120	2.0	0.064			
-	3.33	0.866	15	0.028	120	2.3	0.056			
-	3.33	0.866	15	0.028	120	2.6	0.050			

H (deep sea wave height), T (wave period),  $\alpha$  (deep sea wave angle)

experiments were conducted by changing  $L_G/L_x$  values (Fig. 7). For two groin opening, as the groin length is 100 cm, the greatest amount of accretion (R) is obtained. R values are decreasing from groin length of 100 cm to 133.33 cm.

As can be seen that, the greater  $L_x$ , the smaller are R values. However, this conclusion should not result in a wrong opinion such that “in order to increase the accretion, one must be shortening the groin length”. Because an increase in  $L_x$  will also lead to an increase in protection area ( $A_G$ ). Therefore, one should be aware of the fact that, even though the R values lessen, the total accretion volume will certainly increase.

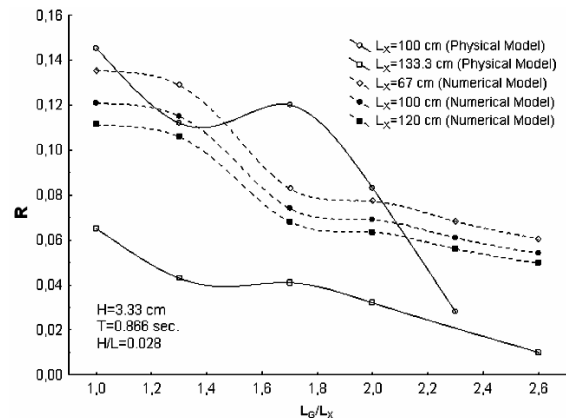


Fig. 7—The effects of groin length on accretion for various groin lengths ( $\alpha=15^\circ$ )

3.1.2. Effect of groin opening ( $L_G$ )

The results of the experiments, the effect of  $L_G$  on  $R$ , are given in Figs. 7 and 8. As can be seen, maximum  $R$  values are obtained when  $L_G/L_X$  is smaller. Two lines in Fig. 7 have similar tendency. Among these lines,  $R$  value is maximum at  $L_X=100$  cm. It is clear that the amount of accretion decreases with the increase in groin opening.

3.1.3. Effect of wave height ( $H$ )

The main reason for alongshore and cross-shore sediment transport is the wave height ( $H$ ). The amount of sediment transported decreases with the decreasing wave height. However, this does not necessarily mean that sediment accumulation is possible every time.

In this study, in order to asses the effect of wave height, two values for wave height are taken, namely 3.33 and 5.33 cm, and the experimental results are given in Fig. 8, which describe the effect of  $H$  on  $R$  imply that if  $H$  goes up,  $R$  values will decrease. Numerical model results are opposite to this result (Fig. 8).

3.1.4. Effect of wave period ( $T$ )

$R$  values for two periods, namely 0.866 sec. and 0.692 sec. were compared and outcomes are given in Fig. 9 with a constant value of  $\alpha_0=15^\circ$ . It can be seen that, an increase in  $T$  values causes an increase in  $R$  values. In other word, the less steep waves, the more accretion.

3.1.5. Effect of wave angle ( $\alpha$ )

Waves with angles to the shoreline are one of the main reasons for shoreline sediment movement. Wave angle is the main factor in designing groins since most of the sediments entering groin protection area formed due to sediments moving along the shoreline. Controlled tests are conducted for two angles ( $\alpha=30^\circ$  and  $\alpha=15^\circ$ ) with other constant parameters, namely  $T=0.866$  sec.,  $L_X=100$  cm and  $H=3.33$  cm, and results obtained are given in Fig. 10. It is obvious that, more  $R$  values are observed in the case of  $\alpha=30^\circ$ .

3.2. Evaluation of numerical model results

The numerical model, used in the prediction of bed topography in the changes in the vicinity of groins, has resulted in similar characteristics as physical model results (Figs. 7-10). Numerical model were performed according to CERC Model for  $x/x_b=0, 0.5$  and  $0.7$ ; and to Kamphuis Model<sup>3</sup> for  $x/x_b=0$ . The

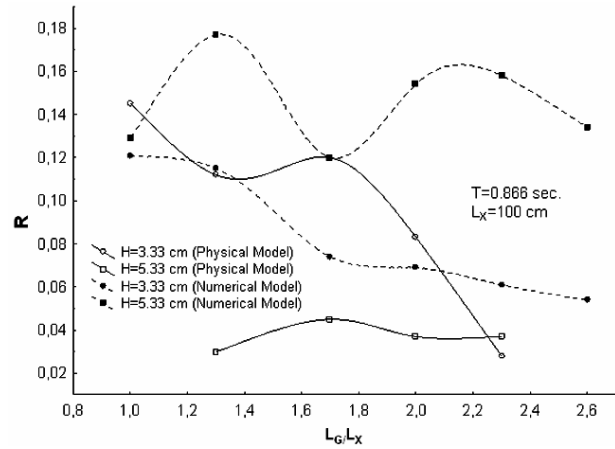


Fig. 8—The effects of wave height on accretion ( $\alpha=15^\circ$ )

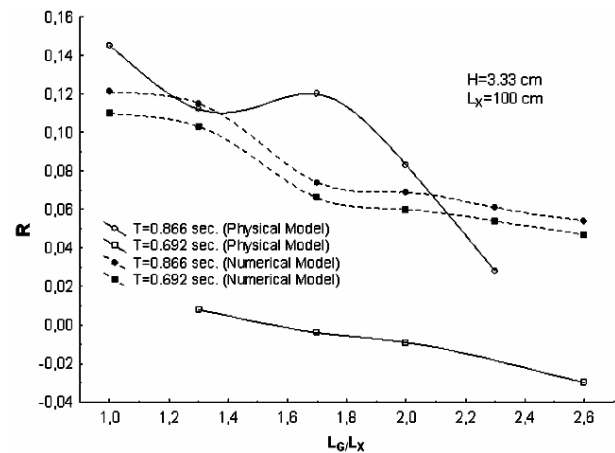


Fig. 9—The effects of wave period on accretion for various groin lengths ( $\alpha=15^\circ$ )

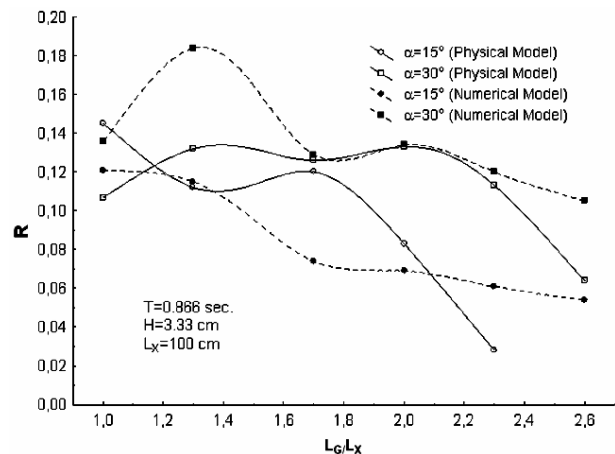


Fig. 10—The effects of wave angle on accretion ( $H=3.33$  cm)

results of these four models are presented in Figs. 11 and 12, in which the variation of R vs.  $L_G/L_X$  was plotted for constant values of  $H=3.33$  cm,  $T=0.866$  sec. and  $\alpha=30^\circ$ . It can be seen that, the greatest R values are obtained by both Kamphuis model and CERC model for  $x/x_b=0$  showing similar results. CERC model for  $x/x_b=0.5$  and  $0.7$  result in relatively small and near R values: By comparing the results of physical and numerical models carried out at the same conditions, it was concluded that, the nearest results between two models were observed by CERC model for  $x/x_b=0$ . Therefore, in the following analyses, only the results of this model are employed. The results of the physical and the numerical models are given in Figs. 7-10 together. It is obvious that, the R values of the physical and numerical models have similar tendency.

**3.3. Analysis of the field study results**

The results of the numerical model and field measurement of R values for a single straight groin (Fig. 6) shows that one groin caused remarkable accretion at the updrift (west) side and some erosion at the downdrift (east) side of the groin. Some erosion has been observed at the head zone of the groin. The field measurements have yielded less accretion than that of the numerical model. The erosion patterns of the measurements and numerical model are similar.

The R values and measurement dates are given in Table 3. Variation of R values is given in Fig. 13. The dimensionless accretion parameter (R) has similar characteristics both in field and numerical model. During the measurement season, there are few

increases in R values in measurements, mainly due to steep waves that caused offshore sediment transport.

**4. Discussion**

In this study, physical and numerical models are conducted in order to investigate the effect of various groin parameters (length and opening) and wave parameters (wave height, wave period and wave

Table 3—R values obtained from field and numerical models (Çarşıbaşı)

Measurement Date	R (Field Measurement)	R (Numerical Model)
11.12.1997	0.007	0.034
04.06.1998	0.021	0.055
10.12.1998	0.036	0.059

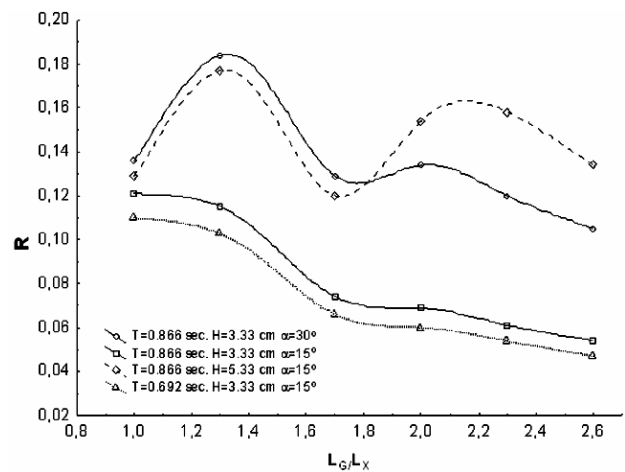


Fig. 12—The results of the tested numerical models

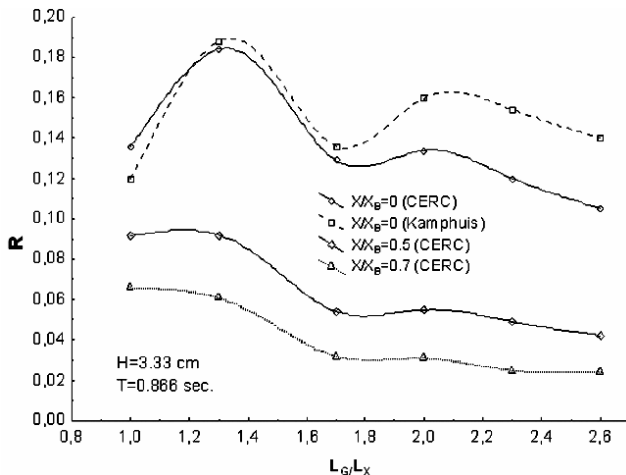


Fig. 11—The results of the tested numerical models ( $\alpha=15^\circ$ )

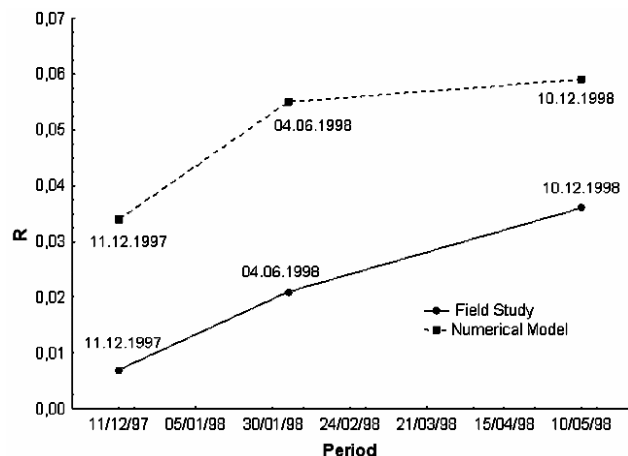


Fig. 13—The variation of R with time (one Groin)



angle) on the dimensionless accretion parameter  $R$  of a region which is protected by straight groins. The results of a numerical model are compared with field data that were obtained by deep sounding measurements at Çarşıbaşı coasts, Trabzon Province, Turkey. The conclusions of this study may be summarized as follows:

The length of groin ( $L_X$ ) was one of the most important factors on variation of accretion parameter ( $R$ ) for groins. For all groin openings, as the groin length is 100 cm, the greatest amount of accretion was obtained. After 100 cm of groin length,  $R$  value has been decreased. However, this does not result in a decrease in total accretion volume; because of the fact that,  $L_X$  also affect the total protection area and consequently,  $R$ .

Another factor to be effective of affecting sediment accretion parameter is the groin opening ( $L_G$ ). According to the results of physical model studies, maximum  $R$  was obtained when the ratio of the opening between two successive groins to the groin length ( $L_G/L_X$ ) is equal near to 1.7, ( $L_G/L_X \cong 1.7$ ). However, this opinion is not supported by the results of numerical model, which implies that the smaller  $L_G/L_X$ , the smaller  $R$ . Since the physical models are more reliable than numerical models (because of more assumptions in the latter), it is recommended that  $L_G/L_X$  is nearly equal to 1.7. In the case of greater values both of wave period and angle, greater accretion is expected and this conclusion is supported both by physical and numerical model results.

According to the experimental results, when  $H$  values goes up, then  $R$  values decrease. In addition, numerical model results are opposite to the experimental results. It is clear that the amount of discharge increases in  $H$  value increase is looking over the test results. However, this case has not been erosion on the beach. Amount of accretion is dependent on both the breaking wave whether or not is in the protection area, and profile which is formed with greater  $H$  value.

Monochromatic waves were reproduced in the model, which resulted in a uniform breaking zone. In nature, spectral wave conditions, with a varying breaker zone along the shoreline, are more representative. During the physical studies, the scale was chosen based on laboratory space and available measuring equipment. Sediment scaling relations have not yet been developed to accurately measure the quantitative movement of sediment.

The aforementioned stipulations, of course, affect the reliability of the results. But, since some conclusions obtained from various studies related to this study are in agreement with these conclusions, it is possible to say the results are useful in planning the preliminary layout for groins. However, more comprehensive field and/or laboratory studies should be conducted relative to this problem, prior to final design of groins.

The numerical model, used in the prediction of bed topography changes in the vicinity of groins, has resulted in similar characteristics as field measurements. However, in order to reach more reliable conclusions, more field data are necessary.

## 5. References

1. Price W.A. & Tomlinson, K.W., The effect of groins on stable beaches, *Proc. of the 11<sup>th</sup> Coastal Eng. Conf.*, 1 (1968) 518-526.
2. Barcelo J.P., Experimental study of hydraulic behaviors of groin system, *Proc. of the 11<sup>th</sup> Coastal Eng. Conf.*, 1 (1968) 526-548.
3. Hanson H. & Kraus, N.C., Comparison of shoreline change with physical and numerical models, *Proc. Coastal Sediment*, 1(1991) 1785-1799.
4. Kraus N.C., Hanson, H. & Blomgren, S.H., Modern functional design of groin system, *Proc. of the 24<sup>th</sup> Coastal Eng. Conf.*, (1994) 1327-1342.
5. Badici P., Kamphuis, J.W. & Hamilton, D.G., Physical experiments on the effects of groins on shore morphology, *Proc. of the 24<sup>th</sup> Coastal Eng. Conf.*, (1994) 1782-1796.
6. Güngördü Ö. & Otay, E.N., Numerical model of shore change, *Advances on Civil Engineering 3<sup>th</sup> Technical Congress*, Ankara, Turkey, (1997) 701-710 (In Turkish).
7. Leont'yev I.O., Short-term shoreline changes due to cross-shore structures: a one line numerical model, *Coast Eng*, 31 (1997) 59-75.
8. Özölçer İ.H., Kömürçü, M.İ., Birben, A.R., Yüksek, Ö. & Karasu, S., Effects of T-shape groin parameters on beach accretion, *Ocean Eng*, 33 (2006) 382-403.
9. Yüksek Ö., Effects of breakwater parameters on shoaling of fishery harbors, *J Waterw, Port, Coast Ocean Eng.*, 121 (1995) 13-22.
10. Özölçer, İ.H., *A study on the effects of groins in shore protection*, Ph.D. thesis, Karadeniz Technical University, Turkey, 1998 (In Turkish).
11. Perlin, M. & Dean, R.G., 3-D Model of bathymetric response to structure, *J Waterw, Harbors, Coast Eng.*, 111 (1985) 153-170.
12. Watanabe, A., Maruyama, K., Shimizu, T. & Sakakiyama, T., Numerical prediction model of three dimensional beach deformation around a structure, *Coastal Eng. Japan*, 29 (1986) 179-193.
13. Larson, M. & Kraus, N.C., *SBEACH: Numerical model for simulating storm-induced beach change*, (US Army Coastal Engineering Research Center) 1989, pp. 269.

14. Watanabe, A., Total rate and distribution of long shore sand transport, *Proc. 23<sup>rd</sup> Coastal Eng. Conf.*, 3 (1992) 2528-2541.
15. CERC, *Shore protection manual*, fourth edition, (US Army Coastal Engineering Research Center), 1984.
16. Hanson, H. & Kraus, N.C., *GENESIS: Generalized model for simulating shoreline change*, Report 1, (US Army Coastal Engineering Research Center), 1989, pp. 25-57.
17. Kraus, N.C. & Harikai, S., Numerical model of the shoreline change at Oarai beach, *Coast Eng*, 7 (1983) 1-28.
18. Kamphuis, W.J., Alongshore sediment transport rate, *J Waterw, Port, Coast Ocean Eng.*, 117 (1991) 624-640.
19. Karasu, S., *The effects of groins on the black sea coast and a numerical model approach*, MSc. thesis, Karadeniz Technical University, Turkey, 1998 (In Turkish).